

The TESLA X-FEL Injector

K. Flöttmann, Ph. Piot*, DESY, Hamburg, Germany

M. Ferrario, LNF-INFN, Frascati, Italy; B. Grigoryan, YerPhi, Yerevan, Armenia

Abstract

The high-brightness beams demanded to drive future short-wavelength SASE FEL-based light sources result in stringent demands on the electron beam source. In the foreseen TESLA X-FEL [1], a slice emittance (over the cooperation length) of less than 1.6 mm-mrd and a rms bunch length of $\sim 25 \mu\text{m}$ (corresponding to a peak current of 5 kA) are required at the undulator entrance. In this paper, we present the conceptual design of the photoinjector system for the TESLA X-FEL including Beam Dynamics studies performed with the codes ASTRA and HOMDYN. The proposed injector can generate 1 nC bunches with mm-mrd transverse emittances and longitudinal emittance of 60 keV-mm at an energy of 140 MeV.

1 OVERVIEW

An overview of the injector [5] layout is presented in Fig. 1. The injector incorporates: a radio-frequency (rf) photoemission gun, a standard TESLA-accelerator module, a 3rd harmonic rf-section, a bunch compressor, and a diagnostics section. The electrons are produced via photoemission using a Cesium Telluride (Cs_2Te) photocathode illuminated by UV light ($\lambda = 262 \text{ nm}$). The injector is required to operate in multibunch mode, that is to generate a train (macropulse) of 11500 bunches spaced by 93 ns (the macropulse repetition rate being 5 Hz). For a 1 nC charge per bunch, the laser must provide 1 μJ of UV light per macropulse.

The simulations presented henceforth were performed using the tracking code ASTRA [2] and the multi-slice model HOMDYN [3]. In this paper we only present simulations for $Q = 1 \text{ nC/bunch}$.

2 BEAM GENERATION & ACCELERATION

The beam generation line consists of an axially symmetric rf 1.625 cell L-band cavity [4] ($f = 1.3 \text{ GHz}$). The cavity electric field on the photocathode, should be as high as possible to provide the highest possible acceleration and thereby reduce the beam blow up imparted by space charge forces. In the present case the emittance blow-up is due to space-charge: rf-induced emittance growth is negligible (at least one order of magnitude lower). It is planned to operate the cavity with a peak E_z -field, of $E_o \sim 60 \text{ MV/m}$ on the cathode.

Given the cavity E_z -field, the free parameters that need to be tuned in order to optimize the beam parameters are:

the photocathode drive-laser rms spot size, σ_r , pulse duration, L_t , and the laser launch phase, ϕ_{rf} . Henceforth a laser with a radially and longitudinally uniform distribution is assumed, deviations from these assumptions results in the laser requirements gathered in Table 1. The pulse length L_t impacts the longitudinal emittance, but also the transverse emittance because of the space charge forces scaling with the current within the bunch. In order to find the optimum setting for σ_r and L_t , we studied the evolution of the beam parameters at $z = 1 \text{ m}$, while scanning σ_r and L_t . Since the emittance at this location is largely due to correlations (which are removed further downstream using the “emittance compensation” scheme), we computed a “reduced” emittance, i.e. an emittance that is calculated after removal of linear and quadratic correlations of r , p_r and z . Fig. 2 compares the emittance and reduced emittance for two different values of ϕ_{rf} . On the other hand, the thermal emittance scales as $\varepsilon_{th} = \frac{\sigma_r}{\sqrt{3}} \sqrt{2K/m_e c^2}$ [6] (K is the average kinetic energy of the emitted electrons). While the thermal emittance calls for the smallest spot size, the reduced emittance has a shallow optimum at about 0.75 mm (for $\phi_{rf} = 44^\circ$), which gives also reasonable values for the projected emittance. Table 1 collects initial parameter settings as obtained after further optimization of the complete beam line. A solenoid is located close to the cathode in order

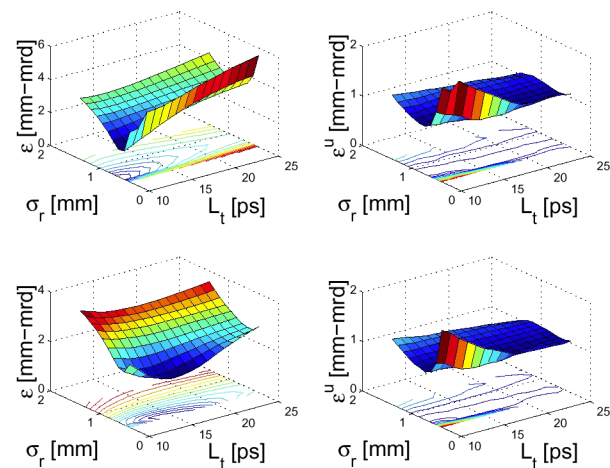


Figure 2: Projected (left column) and “uncorrelated” emittance (right column) dependence versus σ_r and L_t . The computation are performed for $\phi_{rf} = 40^\circ$ (top row) and $\phi_{rf} = 44^\circ$ (bottom row).

to control the beam envelope, which tends to be divergent due to the presence of space charge forces. Though it provides focusing, it also contributes to a reduction of the correlated emittance via the so-called emittance compensation

*PIOT@MAIL.DESY.DE

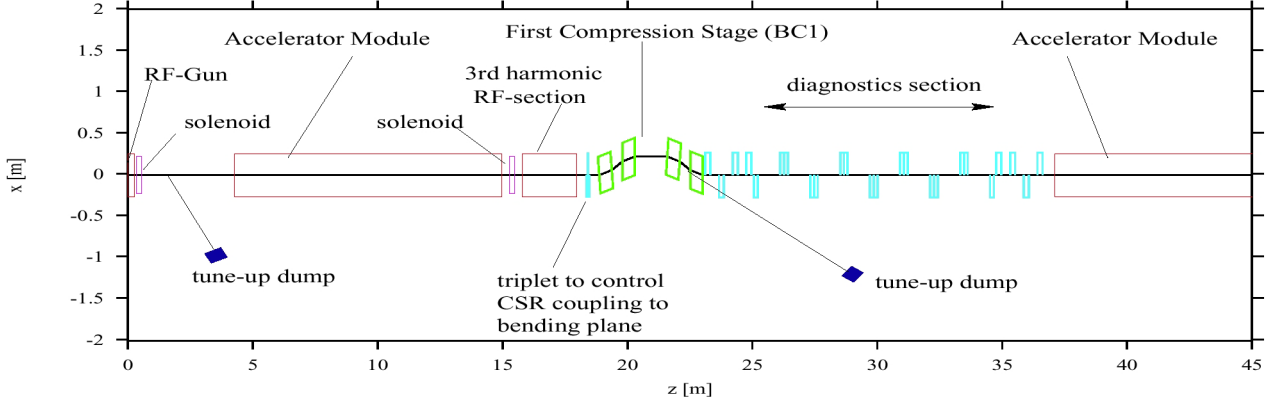


Figure 1: Layout of the X-ray FEL injector at TESLA. The represented elements are rf-cavity (red), dipoles (green), solenoids (violet), and quadrupoles (cyan).

process [7]. The peak B_z -field of the solenoid, the length of the downstream drift and the gradient of the accelerating cavity (booster) are chosen to provide a proper matching condition for the beam. One possible matching technique is based on the so-called “invariant envelope” [8]: The beam should be at a laminar waist at the booster linac entrance (i.e. $\sigma_r' = 0$) and the average energy gradient in the booster $\gamma'_{boost} \doteq \bar{G}_{z,1}/(m_e c^2)$ should be related to the rms beam size σ_w , the incoming mean beam energy γ and the peak current \hat{I} via the relation: $\gamma'_{boost} = \frac{2}{\sigma_w} [\hat{I}/(3I_o\gamma)]^{1/2}$, where I_o is the Alfvén current (17 kA for electrons). In this way, the beam envelope is matched to the “invariant envelope” which has the property to reduce simultaneously the beam spot size and the transverse momentum. In the drift behind the gun and the solenoid the emittance decreases for most parameter settings not to a single minimum, but shows two minima separated by a local maximum [9]. For a certain setting of the solenoid the local maximum of the emittance is located at the position of a waist of the beam envelope. At that point, we locate the booster: a standard TESLA accelerator module that comprises eight superconducting 9-cell cavities ($\bar{G}_{z,1} \simeq 11.5$ MV/m for the first four cavities and 25.0 MV/m for the others). The beam is thereby accelerated up to ~ 160 MeV.

	parameter	nom. value	tolerance	unit
laser	σ_r	0.75	± 0.05	mm
	L_t	20.0	± 1.0	ps
	rise time	-	≤ 2	ps
	Q	1.0	$\pm 10\%$	-
	r -distrib.	Uniform	10%	-
	t -distrib.	Uniform	10%	-
gun	E_o	60	± 0.3	MV/m
	ϕ	44	± 2	°
solen.	\bar{B}	198	± 1	mT

Table 1: Requirements and tolerances on parameters settings for various elements of the electron source.

3 BUNCH COMPRESSION & LONG. PHASE SPACE CORRECTION

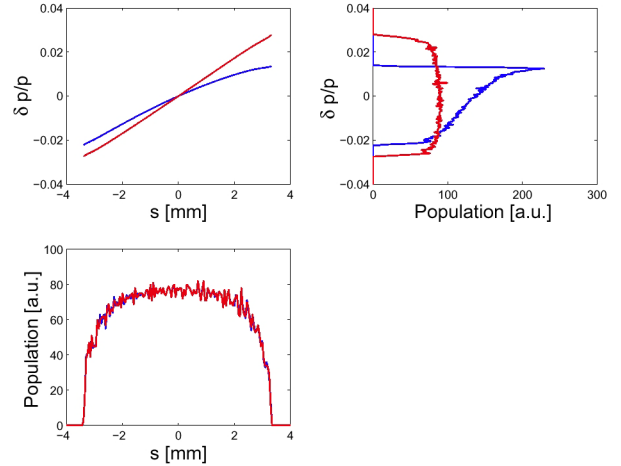


Figure 3: Effect of the 3rd harmonic section on the longitudinal phase space at $z = 18.00$ m.

A general problem inherent to rf guns is the interplay between transverse and longitudinal emittances. To reduce the transverse emittance the bunch length, σ_z , generated in the rf-gun should be made long; this leads to an increased longitudinal emittance. While the increase in the gun might still be tolerable, the longitudinal emittance growth induced by the cosine-like rf potential in the subsequent accelerating section(s) is generally intolerable ($\varepsilon_z \propto \sigma_z^3$). A scheme for compensating the longitudinal phase space (s, δ) nonlinearities introduced during the acceleration consists of using a 3rd harmonic ($f = 3.9$ GHz) accelerating section prior to the first bunch compressor [10]. Two additional advantages of the 3rd harmonic section are: (1) it can also be used to compensate for nonlinearities of the subsequent bunch compressor sections, and (2) it reduces the sensitivity of bunch compression on incoming time jitter. The average energy gain $\bar{G}_{z,3}$ and phase ϕ_3 required

for the correction can be derived analytically, requiring: $d^2\delta/d^2s|_{s=0} = 0$, $d^3\delta/d^3s|_{s=0} = 0$, while $d\delta/ds|_{s=0}$ is adjusted to the desired value (e.g. for maximum compression $d\delta/ds|_{s=0} = -1/R_{56}$). The staged compression scheme, foreseen in TESLA FEL [11], requires an incomplete compression in the first bunch compressor, a four-bend chicane ($R_{56} = -10$ cm) located in the injector downstream of the 3rd harmonic rf-section (which we assume consists of four TESLA cavities frequency-scaled to $f = 3.9$ GHz). A comparison of the longitudinal phase before and after correction using the 3rd harmonic rf-section is presented in Fig. 3. Thus the bunch is compressed from $\sigma_z \sim 2$ mm down to $\sigma_z \sim 0.3$ mm. The 3rd harmonic rf-section parameters were optimized via simulation – using as a starting point the aforementioned set of equations – to achieve a linear longitudinal phase space downstream of the compressor. The obtained values are: $\bar{G}_{z,3} = 13.9$ MV/m and $\phi_3 = -179.26^\circ$ and $\phi_1 = -16.03^\circ$ for the phase of the booster. During the compression process the projected emittance dilutes from 0.9 to 1.1 mm-mrd due to bunch self-interaction via radiative effects [11].

4 DIAGNOSTIC & MATCHING SECTION

Downstream of the compressor a matching section follows: it allows the transverse matching of the beam into the subsequent accelerating sections and also incorporates a diagnostics section. The total length of this section is approximately 10 meters. The optical layout consists of two four-quadrupole telescopes, separated by a FODO channel. The FODO channel comprises four FODO cells with a betatron phase advance, in both plane, of $\mu_{x,y} = 45^\circ/\text{cell}$. Four transverse profile monitors separated by 45° provide an optimum configuration for measuring on-line, with a high resolution, the transverse emittance at the compressor exit.

5 SUMMARY

The evolution of the beam envelope and longitudinal beam parameters along the beam line, up to the 3rd harmonic rf-section are presented in Fig. 4. The achieved parameters upstream and downstream of the bunch compressor are gathered in Table 2.

parameters	at $z=18$ m	at $z=24$ m	units
σ_z	1.8	0.3	mm
σ_E	2.1	2.1	MeV
ε_{tot}	0.9	1.1	mm-mrd
ε_z	58	80	keV-mm

Table 2: Beam parameters downstream of the third harmonic section ($z = 18$ m) and bunch compressor ($z = 24$ m) for nominal settings.

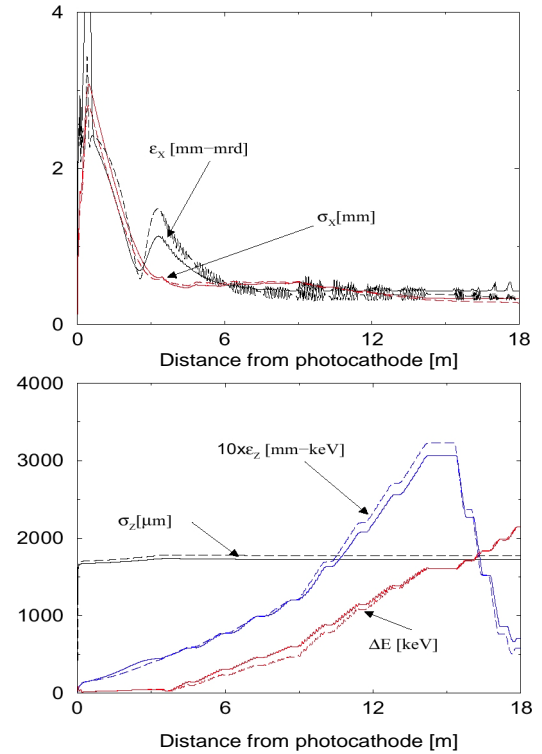


Figure 4: Transverse (**top**) and longitudinal (**bottom**) beam parameters evolution along the injector beamline. The dashed line and solid lines are results from HOMDYN and ASTRA respectively.

6 REFERENCES

- [1] TESLA TDR - TESLA Technical Design Rep., TESLA-01-23, DESY-HH (2001)
- [2] Flöttmann K., *Astra User Manual*
http://www.desy.de/~mpyflo/Astra_dokumentation/
- [3] Ferrario M., Serafini L., EPAC'98, pp.1271-1273 (1998)
- [4] Dwersteg B., Flöttmann K., Sekutowicz J., Stolzenburg Ch., *NIM A393*, pp. 93-95 (1997);
- [5] Ferrario M. Flöttmann K., Grigoryan B., Limberg T., and Piot, Ph., report TESLA-FEL-01-03, DESY-HH (2001)
- [6] Flöttmann K., report TESLA-FEL-97-01, DESY-HH
- [7] Carlsten B.E., *NIM.,A285* pp. 313-319 (1989)
- [8] L. Serafini and J.B. Rosenzweig, *Phys. Rev. E 55* p. 7565 (1997)
- [9] Ferrario M. et al., report SLAC-PUB 9400, (1999)
- [10] Flöttmann K., Limberg T., and Piot, Ph., TESLA-FEL-01-06, DESY-HH (2001); Smith T. I., SLAC report 303, pp. 421-425 (1986); Dowell D., et. al, *NIM A375*, pp. 108-111 (1996)
- [11] Limberg T., and Piot, Ph., "Integrated modeling of the TESLA X-FEL", this conference